RSC Advances

PAPER

View Article Online
View Journal | View Issue

Cite this: *RSC Adv.*, 2025, **15**, 33427

Pesticidal efficacy of some innovative phenyl benzoate-based heterocycles against *Tetranychus urticae* (Koch) and *Spodoptera littoralis* (Boisd.): biochemical aspects and *in silico* studies

Gehad E. Said, *[a] Ehab Abdel-Latif,[a] Adel M. Younis, [a] Tamer K. Khatab[b] and Mohamed E. Mostafa[c]

Received 26th May 2025
Accepted 29th August 2025

DOI: 10.1039/d5ra03713a

rsc.li/rsc-advances

It is very desirable to develop new pesticide lead compounds to reduce the increasing resistance in agricultural pests caused by the widespread usage of agrochemicals. This study assessed the synthesis of novel hydrazones and heterocycles as potential pesticidal agents. The pesticidal efficacy of the synthesized compounds was assessed against *Tetranychus urticae* (Koch) and *Spodoptera littoralis* (Boisd.). Amongst the tested derivatives, compounds **3**, **4**, **10**, **12**, **13**, **16**, and **17** exhibited outstanding activity against 4th instar larvae of *S. littoralis* and adult females of *T. urticae*. The effect of the promising derivatives on some key enzymes of both pests clarified the mode of action of the outstanding derivatives. A molecular docking study was performed for the synthesized compounds against AChE and GST targets, which revealed the good affinity between the tested compounds and the target proteins in comparison with reference ligands. In addition to identifying promising pesticidal candidates, this study provides a robust framework for developing next-generation pest management techniques that tackle resistance issues and promote sustainable agricultural practices.

1. Introduction

Agricultural pests are a worldwide problem causing major losses and are considered the main obstacles limiting the production of cotton.[1–3] The most common pest management strategies in cotton production are based on applying synthetic pesticides, which play a vital role in boosting cotton production.[4] The polyphagous herbivores attacking cotton and causing serious damage in Egypt are the cotton leafworm *Spodoptera littoralis* (Boisduval) and the two-spotted spider mite *Tetranychus urticae* (Koch).[5] Despite the fact that pesticide use has improved crop productivity and provided efficient pest control, the recurrent use of synthetic pesticides has severe consequences on the environment and has caused unintended negative impacts on human health and non-target species besides the rapid emergence of resistant strains. Under these circumstances, ongoing efforts are required to develop novel pesticides with new modes of action for use in agriculture.[6,7]

In particular, cyclic organic frameworks, especially heterocyclic frameworks, are dominant subunits in many pharmaceuticals and agrochemical products due to their intriguing capabilities.[8–10] Several biological activities, including insecticidal, antidiabetic, diuretic, anti-bacterial, anticonvulsant, antifungal, tuberculostatic, anticancer, antiviral, anti-inflammatory, and anti-tumor properties, have been documented in heterocyclic compounds, especially those consisting nitrogen, oxygen and/or sulfur atoms[11–28] (Fig. 1). Many heterocyclic compounds may be constructed using aromatic aldehydes, which are flexible and convenient precursors and may be suitable for addition followed by heterocyclization or cycloaddition with different chemicals to construct heterocycles of various sizes with one or more heteroatoms, which are highly valuable as pharmaceutical drugs.[29–31]

Hydrazone derivatives have gained increasing attention and possess remarkable insecticidal properties with a broad spectrum of action, minimal toxicity, outstanding activity, and simple preparation.[32] Several derivative-based hydrazones with high pesticidal activity have been discovered, such as benzophenone hydrazones,[33] phthalimide hydrazones,[34–36] heterocyclic hydrazones, halohydrazones, thiophosphate hydrazones,[32] metal complex-containing hydrazones[37] and natural product-based hydrazone derivatives.[32,38]

Synthetic hydrazones exhibit insecticidal activity through multiple mechanisms by targeting key physiological processes in insects. Several synthetic hydrazone derivatives can significantly inhibit glutathione S-transferase (GST) activity.[39]

[a]*Chemistry Department, Faculty of Science, Mansoura University, 35516 Mansoura, Egypt. E-mail: gehadsaid@mans.edu.eg*

[b]*Organometallic and Organometalloid Chemistry Department, National Research Centre, 33 ElBehouth St., Dokki, 12622 Giza, Egypt*

[c]*Plant Protection Research Institute, Agriculture Research Center, 12618, Egypt*

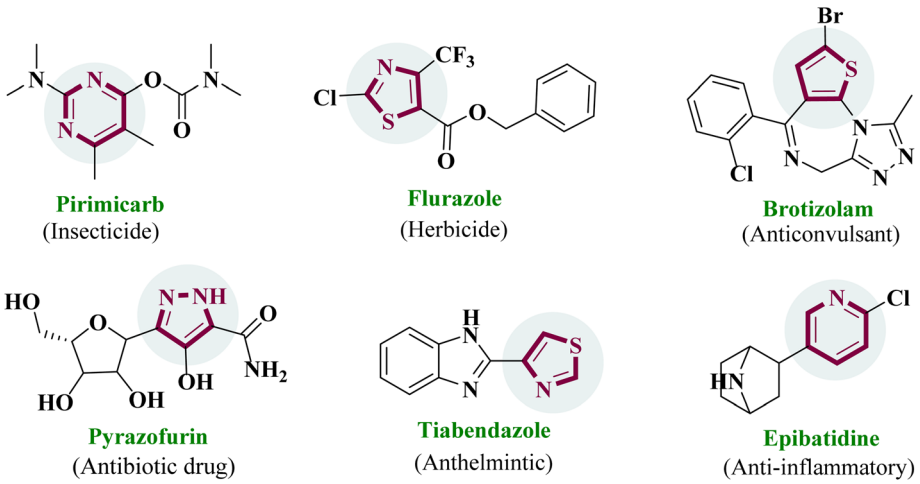

Fig. 1 Some heterocycle-based drugs.

Furthermore, some studies reveal that particular benzoyl hydrazone compounds show strong AChE inhibitory activity, highlighting their promise as effective insecticides.[40] The combined inhibition of GST and AChE by these synthetic compounds suggests a comprehensive strategy for insect control, affecting both detoxification pathways and neural transmission. This multifaceted mechanism of action not only improves the insecticidal effectiveness of these chemicals but also minimizes the risk of resistance development in insect populations.[41]

In summary, with their synthetic accessibility, tunable activity through substitution, unique isomerism, and mode of action profile that either complements or surpasses that of traditional heterocyclic insecticides, hydrazones provide a unique chemical scaffold in the landscape of bioactive heterocycles used as insecticides. Therefore, they are promising insect pest control agents, particularly given that conventional heterocyclic insecticides have drawbacks such as resistance and unfavorable environmental profiles. These differences show that hydrazones are a useful class for creating future agrochemical insecticides.[42,43]

In view of this objective, this study intended to design and synthesize some innovative hydrazones and heterocycles containing a phenyl benzoate scaffold and investigate their efficiency as agrochemical stressors against the cotton leafworm *S. littoralis* and the two-spotted spider mite *T. urticae*. Understanding the mechanistic action of the new leads will be anticipated by investigating the change in the biochemical responses of the targeted pests and studying the docking results.

2. Results and discussion

2.1 Chemical synthesis

The highly versatile 4-formylphenyl benzoate (**1**) was designed according to the reported method[44] and was utilized as a precursor for the construction of a wide variety of hydrazones and heterocycles. The new bis-(arylidene) hydrazine derivative **2** was synthesized through heating of equimolar amounts of **1** and hydrazine hydrate in refluxing ethanol, as depicted in Scheme 1. Using the above-mentioned synthetic methodology, the reaction of **1** with semicarbazide hydrochloride, 2-cyanoacetohydrazide, 4-aminobenzohydrazide, benzene sulfonohydrazide, and isonicotinohydrazide afforded hydrazones **3–7** (Scheme 1), respectively. The new compounds **2–6** were structurally elucidated by elemental and spectroscopic analyses and the results were entirely consistent with the proposed molecular structures. The ^{1}H NMR spectrum of **5** exhibited two singlet signals at 5.82 and 8.46 ppm, which are characteristic of the (NH_2) and (CH=N) protons, respectively. The IR spectrum of compound **6** showed absorption bands at 3195 and 1728 cm^{-1} for the (NH) and (C=O) functional groups, respectively. The SI (Fig. S1–S42) includes a list of the spectral analyses for all the new compounds.

Based on our target to synthesize various heterocycles linked to the phenyl benzoate moiety, 4-substituted benzylidinemalononitrile **8** was prepared.[45] The attempt to synthesize thiazepine phenyl benzoate analogue **9′** *via* the condensation of arylidene **8** with 2-aminothiophenol failed and instead afforded benzothiazole derivative **9** in excellent yield (Scheme 2). A plausible mechanism for the formation of **9** is proposed in Scheme 3. The reaction mechanism involves the Michael addition reaction of 2-aminothiophenol with the 4-substituted benzylidinemalononitrile **8**, giving an intermediate, which in turn converted to benzothiazole **9** through proton transfer and removal of malononitrile as the leaving group. All spectral analyses supported the assigned structure **9** and excluded the other possible structure **9′**. We further investigated the synthesis potential of the 4-substituted benzylidinemalononitrile **8** by examining the Michael addition reactivity with 2-cyanoacetohydrazide as a potential synthetic pathway to obtain diaminopyridinone derivative **10** (Scheme 2). The IR spectrum of compound **10** revealed absorption bands at 3367–3166, 2214, 1737 and 1654 cm^{-1} for the (NH_2), (CN) and (2C=O) functionalities, respectively. Its ^{1}H NMR spectrum exhibited a singlet signal at 5.68 ppm, corresponding to the amino group (NH_2).

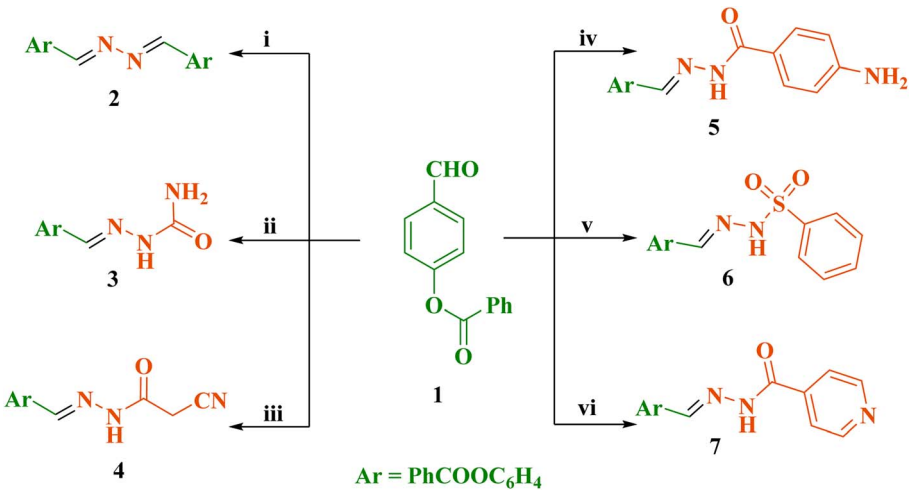

Scheme 1 Reaction conditions and reagents: (i) hydrazine hydrate, abs. EtOH, 30 min; (ii) semicarbazide hydrochloride, abs. EtOH, reflux 30 min; (iii) 2-cyanoacetohydrazide, abs. EtOH, reflux 40 min; (iv) 4-aminobenzohydrazide, abs. EtOH, reflux 30 min; (v) benzene sulfonohydrazide, abs. EtOH, reflux 20 min; (vi) isonicotinohydrazide, abs. EtOH, reflux 15 min.

Introducing the cyanoacetyl moiety was investigated for the construction of various heterocyclic analogues. Cyanoacetyl hydrazone **4** was recently reported by us.[10] In the view of this, treatment of a base-catalyzed solution of **4** in dimethylformamide with phenyl isothiocyanate furnished the intermediate potassium salt **11**, which was then heterocyclized with bromoethylacetate and phenacylchloride to obtain aminothiophene scaffolds **12** and **13** (Scheme 4). The chemical structures of both **12** and **13** have been assigned based on their spectral and elemental analyses. The ^{1}H NMR spectrum of **12** exhibits a triplet signal at 1.22 ppm, quartet signal at 4.15 ppm and singlet signal at 6.69 ppm, which can be assigned to the (CH_3), (CH_2) and (NH_2) protons, respectively. The IR spectrum of **13** exhibited absorption bands at 3448, 3347, 3298 and 3231 cm^{-1}, corresponding to (NH_2, 2NH), and 1734 and 1671 cm^{-1} for the (2C=O) functions.

In view of the diverse pharmacological activities of sulfur heterocycles,[10,46] a bundle of sulphur compounds incorporating the phenyl benzoate nucleus was constructed, as shown in Schemes 4 and 5. The basic-promoted Gewald reaction of **4** with phenyl isothiocyanate and elemental sulfur in ethyl alcohol furnished aminothiazoline derivative **14** (Scheme 5). Additionally, cyclocondensation of cyanoacetyl hydrazone **4** with thioglycolic acid in glacial acetic acid yielded thiazolidin-4-one derivative **15**. Based on both elemental and spectral analyses, the proposed structures of **14** and **15** were also confirmed (*cf.* SI).

Furthermore, Knoevenagel condensation of cyanoacetyl hydrazone **4** with furfural in refluxing ethyl alcohol containing drops of piperidine yielded the arylidene product **16**. Conversely, cyclization of cyanoacetyl hydrazone **4** with salicylaldehyde and 2-hydroxy-1-naphthaldehyde under the same

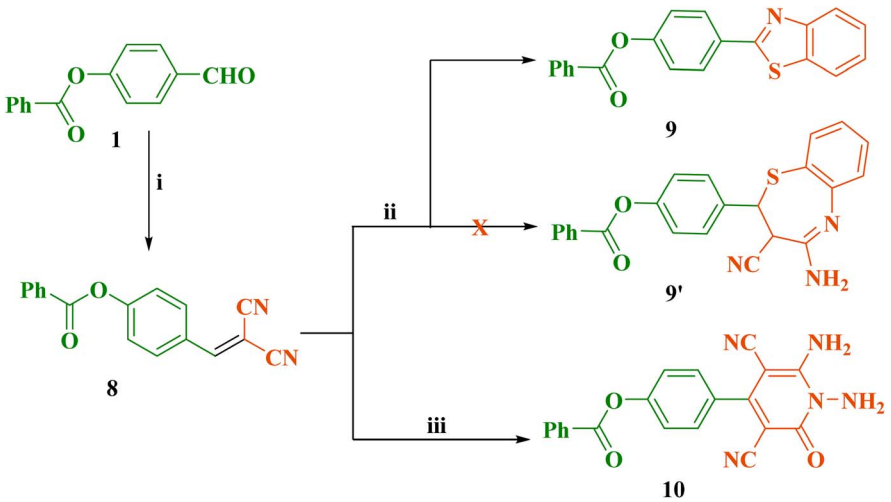

Scheme 2 Reaction conditions and reagents: (i) malononitrile, abs. EtOH, piperidine, 1 h; (ii) 2-aminothiophenol, abs. EtOH, reflux 20 min; (iii) 2-cyanoacetohydrazide, abs. EtOH, piperidine, reflux 10 min.

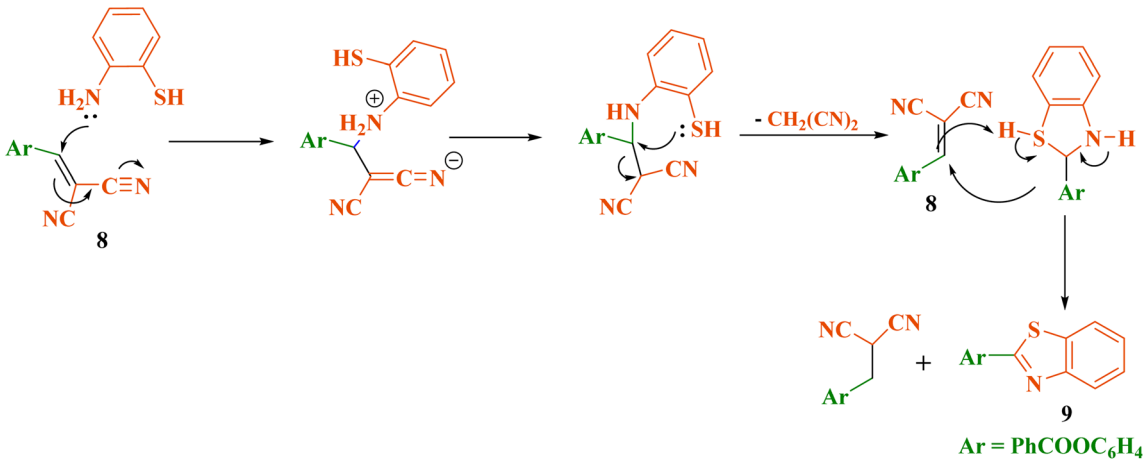

Scheme 3 Plausible mechanism for the formation of benzothiazole compound **9**.

conditions furnished 2-iminochromene and benzochromene compounds **17** and **18**, respectively (Scheme 6). The assignment of the chemical structures of the isolated new compounds was validated using both analytical and spectral data, which confirmed the assigned molecular structures.

2.2 Pesticidal evaluation

2.2.1 Pesticidal activity. The biocidal potential of various heterocyclic systems containing both nitrogen and sulfur has been investigated as profitable pesticidal agents.[31] In the present study, sixteen representative heterocycles containing the phenyl benzoate scaffold have been investigated for their pesticidal efficacy against *S. littoralis* larvae and adult females of *T. urticae* compared with the standard pesticides methomyl and pyridaben.

The laboratory effectiveness of the newly synthesized derivatives against the 4th instar larvae of *S. littoralis* after 24 h of exposure using leaf dip technique (Table 1 and Fig. 2) showed that the standard methomyl was superior based on the toxicity index followed by **13**, **16**, **18**, **17**, **12**, **3**, **5**, **8**, **15**, **9**, **14**, **10**, **4**, **2**, **6** and the least **7**. The lethal concentration (LC_{50}) values were 119.57, 779.82, 1056.90, 1319.40, 1350.68, 1364.14, 1431.10, 1593.38, 1643.05, 1766.59, 1819.64, 2023.41, 2298.45, 2466.63, 2552.63, 3310.98, and 7712.33 ppm, respectively. Comparing the larvicidal activity of the sixteen heterocyclic analogues against the 4th instar larvae of *S. littoralis* after 72 h of exposure (Table 2 and Fig. 2) revealed that the standard reference methomyl was the most effective followed by **3**, **13**, **16**, **17**, **6**, **18**, **9**, **7**, **12**, **10**, **4**, **5**, **15**, **8**, **2**, and **14** with LC_{50} values of 56.28, 243.33, 302.93, 316.30, 406.70, 501.59, 514.64, 540.72, 559.31, 565.10, 583.35, 639.66, 723.09, 734.48, 747.37, 766.84 and 874.48 ppm, respectively.

The acaricidal activity of the sixteen title compounds against the mite-treated adult females of *T. urticae* after 24 h using the leaf dip technique (Table 3 and Fig. 3) was investigated compared with the standard pyridaben. Based on the toxicity index, two groups were observed, where the most acaricidal potency group included the aminothiophene scaffold **13**, arylidene product **16** and the standard reference pyridaben, while the second group was comprised of hydrazone **3**, **17**, **18**, **2**, **12**, **7**,

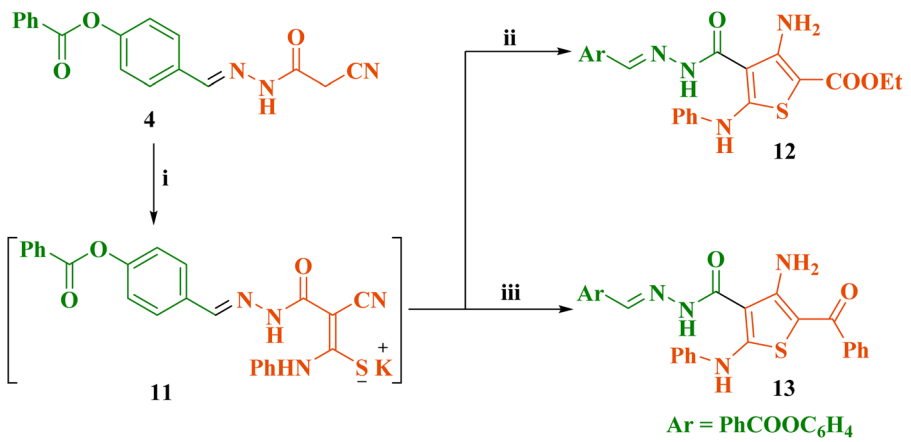

Scheme 4 Reaction conditions and reagents: (i) PhNCS, DMF, KOH, stirring, overnight; (ii) ethyl 2-bromoacetate, stirring, 6 h; (iii) phenacyl chloride, stirring, 6 h.

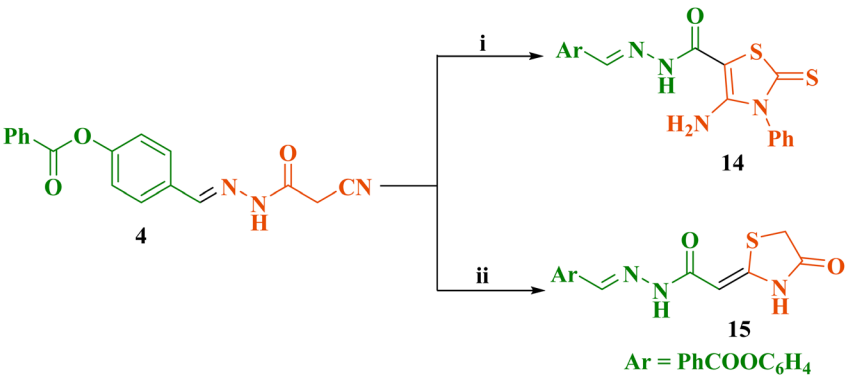

Scheme 5 Reaction conditions and reagents: (i) PhNCS, sulfur, DMF, Et_3N, reflux, 3 h; (ii) thioglycolic acid, glacial AcOH, reflux, 4 h.

10, **9**, **15**, **6**, **8**, **5**, and **14** and the less potent **4**. The recorded LC_{50} values were 524.21, 566.69, 648.71, 2288.96, 2417.29, 2887.60, 3088.10, 3581.59, 3834.56, 3873.01, 4071.67, 5089.62, 6118.36, 6217.41, 7124.54, 8300.53 and 8803.67 ppm, respectively. The susceptibility of the *T. urticae* adult female stage to the newly tested compounds after 72 h (Table 4 and Fig. 3) revealed that aminothiophene scaffold **13** was also the most potent followed by pyridaben, **16**, **18**, **17**, **9**, **3**, **7**, **5**, **10**, **12**, **14**, **2**, **8**, **15**, **4** and the least effective **6**.

Accordingly, by analyzing the overall bioassay results, the most promising heterocycles containing the phenyl benzoate scaffold with a stronger pesticidal effect were aminothiophene scaffolds **12** and **13**, arylidene product **16**, 2-iminochromene **17**, and hydrazones **3** and **4**, beside diaminopyridinone derivative **10**. A broader insecticidal range of various hydrazones containing a benzene ring was previously reported against lepidopteran pests, *S. littoralis* and *S. litura* larvae,[32] which also had an excellent acaricidal effect on *Tetranychus cinnabarinus*.[33] According to our literature survey, hydrazone-containing heterocyclic rings showed effective insecticidal properties against lepidopteran and coleopteran pests.[32]

2.2.2 Effect of the promising compounds on *S. littoralis* and *T. urticae* enzyme level. *In vitro* biochemical estimation of the enzyme activity of *S. littoralis* and *T. urticae* (alanine aminotransferase (ALT), aspartate aminotransferase (AST), glutathione S-transferase (GST) and acetylcholine esterase (AChE)) was performed to clarify the mechanism action of the selected outstanding heterocycles containing the phenyl benzoate scaffold using the median lethal concentration (Tables 5 and 6 and Fig. 4 and 5), respectively.

2.2.2.1 Impact of tested derivatives on the activity of transaminases enzymes in S. littoralis and T. urticae. The change in the transmission enzyme GPT (ALT) activity level of *S. littoralis* was estimated after exposure to the LC_{50} of selected derivatives and listed in Table 5 and Fig. 4 and 5. According to the data, high significant inhibition in the enzyme level ($P < 0.05$) was observed for **10** (−52.19%), followed by **17** (−49.41%), **4** (−38.25%) and **3** (−33.46%), whereas remarkable activation in

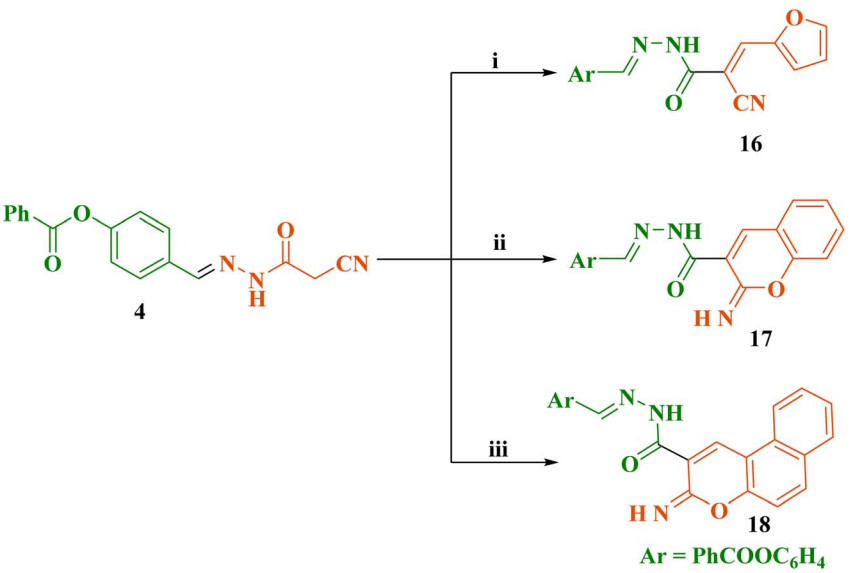

Scheme 6 Reaction conditions and reagents: (i) furfural, abs. EtOH, piperidine, reflux 2 h; (ii) salicylaldehyde, abs. EtOH, piperidine, reflux 1 h; (iii) 2-hydroxy-1-naphthaldehyde, abs. EtOH, piperidine, reflux 1 h.

Table 1 Toxicity of the tested compounds against the 4th instar larvae of *S. littoralis* (Boisd.) after 24 h of treatment under laboratory conditions

		Confidence limit at 95%			Confidence limit at 95%			
Compound	LC_{50} (ppm)	Lower	Upper	LC_{90} (ppm)	Lower	Upper	Slope ± SE	Toxicity index
2	2552.63	2173.18	3000.98	4615.10	3779.56	6488.58	4.983 ± 0.827	4.68
3	1431.10	1125.54	1896.59	4084.82	2751.08	10 181.20	2.814 ± 0.618	8.36
4	2466.63	1771.19	5841.55	9616.89	4604.56	128 885.21	2.169 ± 0.634	4.85
5	1593.38	1071.64	4629.52	10 523.15	3935.58	259 315.99	1.563 ± 0.430	7.50
6	3310.98	1868.64	22 783.80	32 699.2	8477.31	7.41×10^6	1.289 ± 0.401	3.61
7	7712.33	3448.58	122 180.00	1.25×10^5	21 234.53	8.95×10^7	1.061 ± 0.315	1.55
8	1643.05	1359.57	1979.74	3701.29	2909.93	5434.94	3.634 ± 0.533	7.28
9	1819.64	1503.90	2344.67	3993.96	2912.99	7715.52	3.754 ± 0.745	6.57
10	2298.45	1700.31	4553.04	8174.13	4261.19	64 400.97	2.326 ± 0.638	5.20
12	1364.14	1105.51	1755.55	3664.60	2607.81	6763.01	2.986 ± 0.492	8.77
13	779.82	566.17	1042.53	3405.54	2163.79	8620.72	2.002 ± 0.391	15.33
14	2023.41	1581.34	2805.27	7016.28	4470.19	16 862.09	2.373 ± 0.423	5.91
15	1766.59	1397.89	2497.86	4985.99	3223.52	14 278.43	2.844 ± 0.641	6.77
16	1056.90	722.84	1411.41	3857.72	2448.67	13 605.18	2.279 ± 0.590	11.31
17	1350.68	931.37	2098.06	6339.31	3306.17	66 202.32	1.909 ± 0.572	8.85
18	1319.40	846.73	3965.99	8805.50	3234.11	189 177.26	1.555 ± 0.413	9.06
Methomyl	119.57	91.42	174.98	459.04	274.14	1345.32	2.194 ± 0.423	100.00

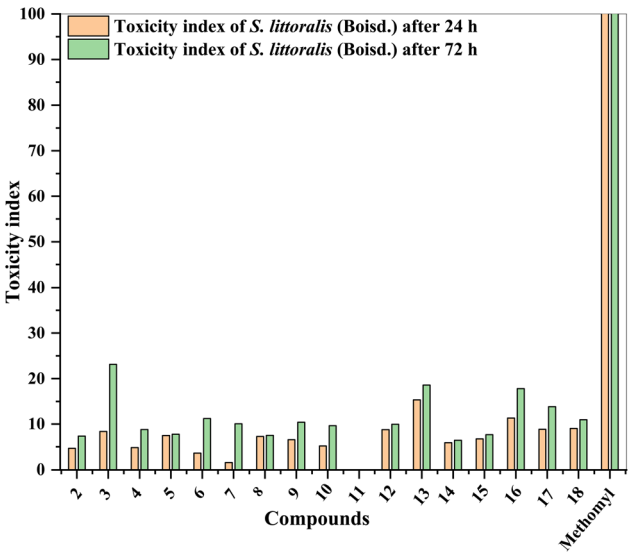

Fig. 2 Toxicity indexes of the tested compounds against *S. littoralis*.

the enzyme level was recorded for **13** (54.18%) and moderate activation for **16** (21.91%) and **12** (10.76%), respectively, compared with untreated insects. Conversely, all the tested toxicants showed a different degree of inhibition of the GPT enzyme level of *T. urticae*. Compounds **3** (−79.84%), **4** (−75.97%), **10** (−73.75%), **12** (−68.24%) and **13** (−64.92%) exhibited the highest inhibition activity and **16** (−38.95%) and **17** (−13.54%) moderate activity, respectively, compared with the control group. All the tested treatments caused significant inhibition in the GOT (AST) enzyme level for **4** (−47.86%), **13** (−39.62%), **16** (−33.57%), **10** (−31.58%), **3** (−9.24%) and **17** (−6.95%), respectively, except for **12** (14.40%), while in the case of *T. urticae*, statistical significant inhibition in the GOT (AST) enzyme level was recorded for all the tested toxicants ranging from **4** (−66.12%) to **3** (−37.25%) compared with the untreated group. Any toxicant that enters an insect's body has an immediate impact on its physiological, metabolic, and reproductive processes, and it drastically alters these processes compared to the control followed by a shift in the level of ALT and AST enzymes.[47,48]

2.2.2.2 Impact of tested derivatives on the activity of some detoxifying enzymes in S. littoralis and T. urticae. GST and AChE are the main groups of detoxifying enzymes that are associated with the development of resistance and used as biomarkers for environmental quality and insecticide resistance monitoring.[49] The data presented in Table 6 and Fig. 4 and 5 exhibited that the GST detoxifying enzyme level of *S. littoralis* was significantly reduced with LC_{50} of **10** (−23.53%), **4** (−13.90%), **13** (−11.76%), **17** (−3.03%) and **3** (−2.14%) and significantly activated for **16** (75.04%) and **12** (8.73%), respectively, compared with the control. Also, the GST level in *T. urticae* recorded remarkable inhibition for **17** (−41.44%), **13** (−36.64%) and **3** (−28.48%) and a significant increase for **10** (67.68%) and **12** (29.92%), **16** (25.60%) and **4** (3.84%), respectively, compared with the untreated pests. The change in the level of AChE of *S. littoralis* hemolymph is tabulated in Table 6 and Fig. 4 and 5, where all the outstanding compounds showed significant inhibition ranging from **13** (−77.56%) to the lowest **12** (−24.01%). Also, for AChE of *T. urticae*, notable significant inhibition was observed for **17** (−28.15%), **13** (−25.22%) and **16** (−17.46%), slight inhibition for **12** (−4.03%) and **4** (−0.29%) and moderate activation for **3** (12.03%) and **10** (11.63%), respectively, compared with the control.

The main biological function of AChE, a serine hydrolase that is a member of the esterase family, is to rapidly terminate the neuronal impulse that happens when ACh enters the synaptic cleft.[47] Our findings are consistent with numerous prior studies that established the potency of hydrazone derivatives, where hydrazones of 1,3-diaminoguanidine,

Table 2 Toxicity of the tested compounds against the 4th instar larvae of *S. littoralis* (Boisd.) after 72 h of treatment under laboratory conditions

Compound	LC_{50} (ppm)	Confidence limit at 95%		LC_{90} (ppm)	Confidence limit at 95%		Slope ± SE	Toxicity index
		Lower	Upper		Lower	Upper		
2	766.84	648.43	921.17	1472.91	1168.03	2245.65	4.521 ± 0.791	7.34
3	243.33	75.84	351.82	1333.78	827.03	7726.97	1.735 ± 0.545	23.13
4	639.66	551.82	756.99	1446.68	1145.04	2092.78	3.627 ± 0.485	8.80
5	723.09	413.44	954.35	2372.48	1675.29	5772.05	2.484 ± 0.643	7.78
6	501.59	351.65	651.38	1632.09	1102.69	4349.11	2.501 ± 0.604	11.22
7	559.31	461.62	669.92	1153.79	913.75	1754.51	4.075 ± 0.72	10.06
8	747.37	606.51	955.11	1831.78	1315.62	3649.34	3.292 ± 0.655	7.53
9	540.72	408.58	685.40	1524.94	1082.22	3269.53	2.846 ± 0.620	10.41
10	583.35	475.38	708.98	1295.07	998.38	2110.62	3.700 ± 0.680	9.65
12	565.10	466.17	680.59	1161.66	913.08	1814.64	4.095 ± 0.748	9.96
13	302.93	186.79	388.39	1035.24	735.97	2436.84	2.401 ± 0.592	18.58
14	874.48	711.22	1074.40	2229.86	1690.81	3519.90	3.153 ± 0.477	6.44
15	734.48	619.49	882.05	1430.80	1133.42	2179.01	4.425 ± 0.769	7.66
16	316.30	185.23	409.56	851.24	645.49	1584.70	2.981 ± 0.743	17.79
17	406.70	328.00	481.26	773.99	630.63	1134.83	4.586 ± 0.902	13.84
18	514.64	398.49	669.65	1818.72	1181.63	4947.59	2.338 ± 0.509	10.94
Methomyl	56.28	42.22	76.16	280.05	175.44	639.02	1.839 ± 0.291	100.00

nitroaminoguanidine, aminoguanidine, and (thio)semicarbazide demonstrated strong to moderate inhibitory effects on both AChE and butyrylcholinesterase BuChE with varying selectivity based on the pattern of substitution.[50] Also, hydrazide–hydrazones and trifluoromethyl compounds considered to be potent inhibitors for AChE and BuChE with IC_{50} values of 19.1–881.1 μM and 46.8–137.7 μM for BuChE and AChE, respectively.[51] Alternatively, the hydrazone derivatives [2-(4-chlorophenyl)- and 2-(3-fluorophenyl)-6-[(4-trifluoromethylphenyl)hydrazonomethyl]furo[3,2-*h*]chromen-5-one] possess abilities to inhibit the catalytic activity of BChE as well as the catalytic and peripheral anionic sites of AChE.[52] Glutathione S-transferases (GSTs) are present in both prokaryotic and eukaryotic cells and assist in protecting cells from toxins, oxidative stress, and other xenobiotics. Pesticide resistance is associated with GST conjugates, which detoxify glutathione to xenobiotics.[2]

2.3 Molecular docking analysis of the tested compounds

Molecular docking is a computational technique that predicts the manner in which two molecules such as a receptor and a ligand bind to form a stable complex. It also determines the optimal orientation of the ligand when it is bound to the receptor and forecasts the degree of their interaction, otherwise referred to as binding affinity. It is a valuable technique for the study of molecular interactions that are the basis of significant

Table 3 Toxicity of the tested compounds against adult females of *T. urticae* (Koch) after 24 h of treatment under laboratory conditions

Compound	LC_{50} (ppm)	Confidence limit at 95%		LC_{90} (ppm)	Confidence limit at 95%		Slope ± SE	Toxicity index
		Lower	Upper		Lower	Upper		
2	3088.10	2061.02	6775.67	27 262.39	10 220.88	609 545.51	1.355 ± 0.37	16.98
3	2288.96	1621.31	3728.55	16 933.50	8191.11	76 931.07	1.475 ± 0.28	22.90
4	8803.67	4164.15	91 565.58	1.56×10^5	28 439.21	6.38×10^7	1.026 ± 0.296	5.95
5	7124.54	3556.69	44 989.65	84 015.03	19 869.42	6.92×10^6	1.196 ± 0.317	7.36
6	6118.36	2826.86	51 174.58	3.97×10^5	48 730.21	4.67×10^8	0.707 ± 0.198	8.57
7	3834.56	2179.51	15 330.21	84 135.94	18 921.38	1.10×10^7	0.956 ± 0.264	13.67
8	6217.41	3038.18	49 180.01	1.42×10^5	25 636.11	6.68×10^7	0.943 ± 0.276	8.43
9	4071.67	2122.58	29 887.15	1.51×10^5	23 596.20	3.28×10^8	0.817 ± 0.258	12.87
10	3873.01	1889.42	37 035.85	1.06×10^5	17 158.79	9.99×10^7	0.891 ± 0.267	13.54
12	3581.59	2687.02	5689.23	14 160.12	7964.30	50 390.14	2.147 ± 0.436	14.64
13	524.21	340.04	716.95	2138.41	1287.07	10 222.22	2.099 ± 0.582	100.00
14	8300.53	3868.63	100 960.0	1.80×10^5	29 642.36	1.53×10^8	0.958 ± 0.286	6.32
15	5089.62	3270.47	12 325.37	35 716.88	14 029.61	330 028.68	1.515 ± 0.327	10.30
16	566.69	1749.45	4530.83	9223.70	2851.76	36 360.31	2.204 ± 0.489	92.50
17	2417.29	1768.20	7655.23	51 144.43	4808.71	44 860.77	1.027 ± 0.262	21.69
18	2887.60	357.99	3152.78	7195.99	14 469.24	2.00×10^6	1.226 ± 0.316	18.15
Pyridaben	648.71	2061.02	6775.67	27 262.39	1894.34	378 359.55	1.355 ± 0.37	80.81

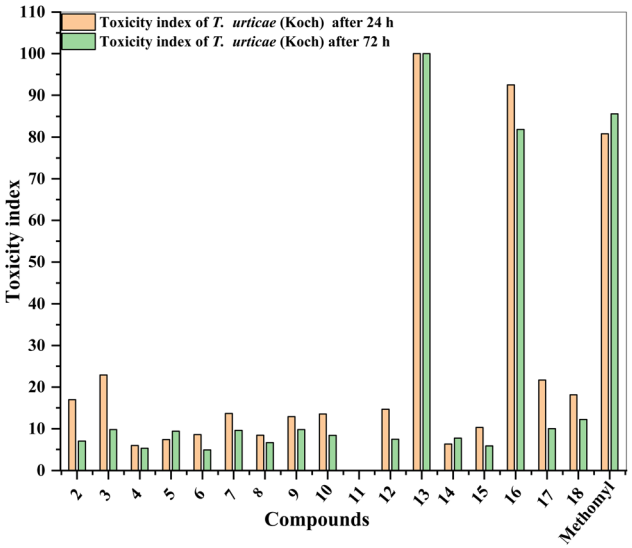

Fig. 3 Toxicity indexes of the tested compounds against *T. urticae*.

biological processes such as enzyme catalysis, signal transduction, and drug action.[53] Molecular docking is also the basis of structure-based drug design given that it makes it possible for researchers to screen and identify potential drug candidates with the binding ability to a target protein, thereby making the discovery of new drugs possible.[54]

The molecular docking results (Table 7) against the AChE target showed that all the tested compounds had good binding affinities with docking scores ranging from −5.77 to −7.93 kcal mol^{-1}. Specifically, compound **12** possessed the best binding affinity (−7.93 kcal mol^{-1}), followed by compounds **13** (−7.49 kcal mol^{-1}) and **18** (−7.26 kcal mol^{-1}), and the native ligand possessed the best interaction score of −8.63 kcal mol^{-1}. The most significant amino acid residues involved in the interaction were ARG17, LEU62, ILE161, LEU496, VAL21, ASN163, and TYR498, which implies that they are highly significant positions for ligand binding. Various types of non-covalent interactions such as hydrogen bonding (donor and acceptor) and Pi–H interactions existed, with distances ranging from 2.86 to 4.32 Å. Few compounds have more than one hydrogen bond and their binding affinity was enhanced as in compound **12**, which formed H-donor interactions with TYR498 and Pi–H with ILE82 (Fig. 6).

In the case of docking against the GST target, good binding affinity ranging from −6.18 to −7.90 kcal mol^{-1}, which are greater than that of the native ligand (−6.31 kcal mol^{-1}) in some cases (Table 8). Compound **13** had the best binding affinity (−7.90 kcal mol^{-1}), followed by compounds **12** (−7.57 kcal mol^{-1}), **17** (−6.89 kcal mol^{-1}), and **6** (−6.89 kcal mol^{-1}). These molecules are comprised of multiple hydrogen bond interactions with significant residues such as GLN74, TYR118, LYS43, ASN59, and TRP8, which are encountered ubiquitously in high-affinity complexes and perform a significant function in ligand recognition. Compound **13** is comprised of hydrogen bonds as well as Pi–cation interactions with residues such as LYS43 and VAL76 and presented a strong and stable binding mode (Fig. 7). Most of the contacts had the appropriate hydrogen bonding distances (2.9–3.5 Å), and a few compounds had more than one simultaneous contact, strengthening their binding strength. These findings suggest that the tested molecules possess favorable binding orientations and interactions in the GST active site.

Fig. S46 and S47 illustrate the validation of docking against the AChE and GST targets upon superimposition of the native (blue) and redocked (pink) poses of the ligands, respectively. The close similarity in the spatial location for both structures with RMSD values of 1.98 Å for AChE and 1.86 Å for GST confirms the accuracy and reproducibility of the docking protocol.

Table 4 Toxicity of the tested compounds against adult females of *T. urticae* (Koch) after 72 h of treatment under laboratory conditions

		Confidence limit at 95%			Confidence limit at 95%			
Compound	LC_{50} (ppm)	Lower	Upper	LC_{90} (ppm)	Lower	Upper	Slope ± SE	Toxicity index
2	1586.90	1092.43	2464.24	14 343.96	6843.28	70 940.34	1.340 ± 0.267	6.99
3	1137.20	759.95	1659.50	9878.54	5123.65	39 151.45	1.365 ± 0.267	9.76
4	2092.64	1474.81	3374.81	16 448.84	7889.64	77 262.17	1.431 ± 0.275	5.30
5	1181.10	822.96	1780.12	7469.42	4013.79	26 335.25	1.600 ± 0.303	9.39
6	2278.02	1224.25	9759.03	67 475.25	13 274.40	4.14×10^7	0.871 ± 0.270	4.87
7	1159.57	760.20	1729.33	11 270.82	5546.39	53 068.04	1.298 ± 0.264	9.57
8	1662.77	1108.57	3808.84	14 226.37	5303.39	316 774.22	1.375 ± 0.373	6.67
9	1135.01	559.90	2119.17	33 940.44	9482.77	2.76×10^6	0.868 ± 0.251	9.78
10	1319.79	798.26	1895.89	9161.51	4905.48	46 531.00	1.523 ± 0.371	8.41
12	1482.69	1052.43	2167.59	10 775.48	5750.16	37 755.65	1.488 ± 0.273	7.48
13	110.94	18.86	204.30	1241.37	738.82	4910.74	1.222 ± 0.338	100.00
14	1436.80	971.05	2216.12	13 891.65	6560.72	72 356.05	1.301 ± 0.265	7.72
15	1894.94	1336.92	2974.62	14 967.54	7323.59	66 653.53	1.428 ± 0.273	5.86
16	135.53	40.79	215.51	901.35	569.96	2923.46	1.558 ± 0.419	81.86
17	1106.53	801.37	1499.68	6162.19	3820.62	14 601.88	1.718 ± 0.284	10.03
18	908.77	593.21	1288.82	7167.38	4013.33	23 084.35	1.429 ± 0.272	12.21
Pyridaben	129.59	85.74	219.45	1402.06	594.16	10 518.32	1.239 ± 0.268	85.61

Table 5 Effect of the LC_{50} of the most potent compounds on the activity of transaminases of both tested pests[a]

	S. littoralis				*T. urticae*			
Compound	GPT (ALT) (U per L) ± SE	Change%	GOT (AST) (U per L) ± SE	Change%	GPT (ALT) (U per L) ± SE	Change%	GOT (AST) (U per L) ± SE	Change%
Control	83.67 ± 1.45^{d}		335.67 ± 3.18^{b}		120.67 ± 3.18^{a}		326.67 ± 2.33^{a}	
3	55.67 ± 0.67^{e}	−33.46	304.67 ± 1.45^{d}	−9.24	24.33 ± 0.88^{f}	−79.84	205.00 ± 2.31^{b}	−37.25
4	51.67 ± 1.20^{e}	−38.25	175.00 ± 1.73^{g}	−47.86	29.00 ± 0.58^{e}	−75.97	110.67 ± 1.76^{g}	−66.12
10	40.00 ± 1.15^{f}	−52.19	229.67 ± 3.18^{e}	−31.58	31.67 ± 1.45^{e}	−73.75	147.00 ± 1.15^{e}	−55.00
12	92.67 ± 1.45^{c}	10.76	384.00 ± 2.89^{a}	14.40	38.33 ± 1.45^{d}	−68.24	179.33 ± 2.33^{c}	−45.10
13	129.00 ± 1.73^{a}	54.18	202.67 ± 2.90^{f}	−39.62	42.33 ± 1.45^{d}	−64.92	137.33 ± 2.91^{f}	−57.96
16	102.00 ± 1.15^{b}	21.91	223.00 ± 1.73^{e}	−33.57	73.67 ± 0.67^{c}	−38.95	155.33 ± 3.17^{d}	−52.45
17	42.33 ± 1.76^{f}	−49.41	312.33 ± 1.45^{c}	−6.95	104.33 ± 0.88^{b}	−13.54	132.33 ± 2.03^{f}	−59.49
$LSD_{0.05}$	4.090		7.284		4.593		6.977	

[a] $LSD_{0.05}$ indicates least significant difference at $p < 0.05$. The figures superscripted with same letters in the same columns do not significantly differ from each other according to Duncan's multiple range test.

Table 6 Effect of the LC_{50} of the most potent compounds on the activity of AChE and GST of both tested pests[a]

	S. littoralis				*T. urticae*			
Compound	GST activity (mmol sub. conjugated per min per mg protein) ± SE	Change%	AChE activity (μg AchBr per min per g b wt) ± SE	Change%	GST activity (mmol sub. conjugated per min per mg protein) ± SE	Change%	AChE activity (μg AchBr per min per g b wt) ± SE	Change%
Control	5.61 ± 0.04^{c}		169.33 ± 2.91^{a}		6.25 ± 0.03^{e}		151.29 ± 4.15^{b}	
3	5.49 ± 0.01^{d}	−2.14	107.67 ± 1.20^{de}	−36.41	4.47 ± 0.01^{f}	−28.48	169.49 ± 5.59^{a}	12.03
4	4.83 ± 0.01^{f}	−13.90	112.00 ± 2.08^{cd}	−33.86	6.49 ± 0.04^{d}	3.84	150.85 ± 6.43^{b}	−0.29
10	4.29 ± 0.01^{g}	−23.53	114.33 ± 2.60^{c}	−32.48	10.48 ± 0.03^{a}	67.68	168.89 ± 2.22^{a}	11.63
12	6.10 ± 0.01^{b}	8.73	128.67 ± 0.88^{b}	−24.01	8.12 ± 0.02^{b}	29.92	145.20 ± 7.29^{b}	−4.03
13	4.95 ± 0.01^{e}	−11.76	38.00 ± 1.73^{g}	−77.56	3.96 ± 0.04^{g}	−36.64	113.13 ± 3.38^{cd}	−25.22
16	9.82 ± 0.01^{a}	75.04	73.33 ± 1.76^{f}	−56.69	7.85 ± 0.02^{c}	25.60	124.88 ± 1.84^{c}	−17.46
17	5.44 ± 0.01^{d}	−3.03	105.67 ± 1.76^{e}	−37.60	3.66 ± 0.04^{h}	−41.44	108.70 ± 3.14^{d}	−28.15
$LSD_{0.05}$	0.048		5.902		0.090		13.927	

[a] $LSD_{0.05}$ indicates least significant difference at $p < 0.05$. The figures superscripted with same letters in the same columns do not significantly differ from each other according to Duncan's multiple range test.

Compound **12** possessed the highest docking score (−7.93 kcal mol^{-1}) against AChE and demonstrated the highest inhibition (approximately 80% inhibition) in both organisms consistently, followed by compounds **13**, **16**, **17**, and **4**, which also exhibited the highest inhibition respective of their docking scores, indicating the strong correlation between the *in silico* findings and the observed activity against *S. littoralis* and *T. urticae*. Conversely, although compounds **3**, **4**, **13**, and **16** were weakly inhibitory against GST by their binding prediction, compound **12**, having the top docking score in GST (−7.90 kcal mol^{-1}), surprisingly acted as a potent GST activator (increasing activity by ∼80% in *S. littoralis* and ∼60% in *T. urticae*). This highlights that strong binding anticipated by docking is not always equal to inhibition but might reflect activation, pointing to the need for experimental verification to completely understand the functional implication of ligand–protein interactions.

Notably, certain discrepancies were observed between the *in silico* docking predictions and the *in vitro* enzymatic responses. Compound **13**, which exhibited high docking scores and strong field efficacy, caused significant activation of ALT in *S. littoralis*.

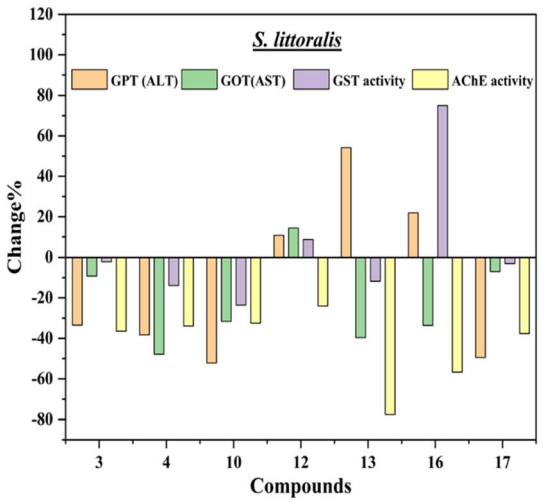

Fig. 4 Effect of the LC_{50} of the most potent compounds on the activity of some selected enzymes in *S. littoralis*.

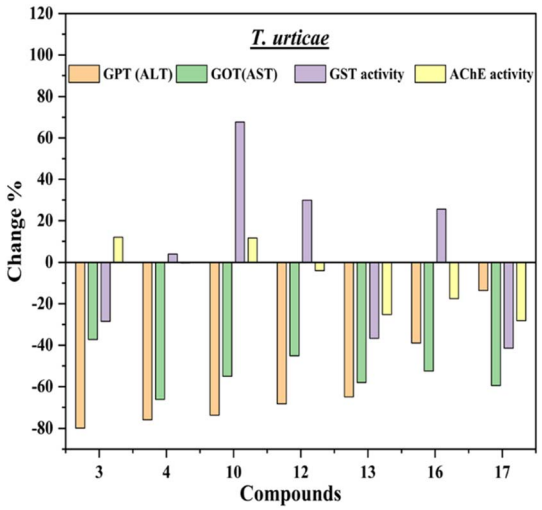

Fig. 5 Effect of the LC_{50} of the most potent compounds on the activity of some selected enzymes in *T. urticae*.

Similarly, compound **12**, predicted by docking to inhibit GST, elicited GST activation in both target species. These outcomes may arise from alternative binding modes within the active or allosteric sites, enzyme conformational stabilization, or compensatory upregulation of detoxifying pathways *in vivo*. These findings highlight that high-affinity binding does not invariably result in inhibition and emphasize the importance of integrating biochemical assays with computational predictions to capture the full functional spectrum of ligand–enzyme interactions in complex biological systems.

3. Experimental

3.1 Chemistry

Instrumental data that described the devices employed in the chemical part were documented in the SI. The preparation of compounds **1**,[44] **4** (ref. 10) and **8** (ref. 45) was performed as previously reported.

3.1.1 Synthesis of hydrazine derivatives 2–7. Equimolar quantities of 4-formylphenyl benzoate (**1**) (1.13 g, 0.005 mol) and hydrazine hydrate (0.48 mL, 0.015 mol, 80%), semicarbazide hydrochloride (0.56 g), 2-cyanoacetohydrazide (0.49 g), 4-aminobenzohydrazide (0.75 g), benzenesulfonohydrazide (0.86 g), or isonicotinohydrazide (0.68 g) were refluxed in ethyl alcohol for 15–40 min. The product was obtained after cooling and washing the mixture with ethanol and drying, yielding the targeted hydrazine derivatives **2–7** without further purification.

3.1.1.1 (Hydrazine-1,2-diylidenebis(methaneylylidene)) bis(4,1-phenylene)dibenzoate (2). Off-white crystals; yield 70%; m.p. = 230–232 °C. IR (ν_{max}/cm^{-1}): 1731 (2C=O$_{ester}$), 1625 (2C=N). ^{1}H NMR (400 MHz) ($CDCl_3$): δ (ppm) = 7.43 (t, J = 7.60 Hz, 2H), 7.56 (t, J = 7.60 Hz, 5H), 7.69 (t, J = 7.60 Hz, 2H), 7.99 (d, J = 8.40 Hz, 1H), 8.12 (d, J = 8.00 Hz, 3H), 8.23 (d, J = 7.20 Hz, 5H), 8.99 (s, 2H, 2CH=N). ^{13}C NMR (100 MHz) (δ/

Table 7 Interactions of tested compounds with AChE target

Receptor residues	Compound	Score (kcal mol^{-1})	RMSD (Å)	Atom of compound	Atom of receptor	Involved residue	Type of interaction	Distance (Å)	E (kcal mol^{-1})
AChE residues involved:	**2**	−6.96	1.68	O22	NH1	ARG17	H-acceptor	2.87	−1.7
ARG17 VAL19 VAL28				O22	NH2	ARG17	H-acceptor	3.06	−2.5
THR30 LEU62 GLU81				6-Ring	CD1	LEU62	Pi–H	3.95	−0.7
ILE82 TRP83 ASN84				6-Ring	CD1	LEU62	Pi–H	4.32	−0.05
ASN86 THR87 ASN97	**3**	−5.77	2.24	N3	OD1	ASN163	H-donor	3.06	−1.6
TRP99 ALA157 THR158	**4**	−6.23	1.83	6-Ring	CD1	LEU496	Pi–H	4.36	−0.5
LEU159 ASP160	**5**	−6.17	1.92	6-Ring	ND2	ASN163	Pi–H	3.87	−0.5
ILE161 TYR162 ASN163	**6**	−6.68	1.91	O6	CA	ILE161	H-acceptor	3.27	−0.6
ASP165 ILE166	**7**	−6.21	2.58	O19	NH1	Arg17	H-acceptor	2.89	−3.3
GLU 485 GLN490	**9**	−6.00	1.61	O11	ND2	ASN493	H-acceptor	2.93	−1.0
ASN493 LEU496 TYR498				6-Ring	CD1	LEU496	Pi–H	4.27	−0.7
	10	−6.00	2.55	N23	O	THR20	H-donor	3.21	−0.8
				6-Ring	CG2	VAL21	Pi–H	4.27	−0.6
	12	−7.93	2.29	N20	OH	TYR498	H-donor	3.02	−0.6
				6-Ring	CB	ILE82	Pi–H	3.63	−0.5
	13	−7.49	1.72	O23	NH1	ARG17	H-acceptor	3.07	−3.5
				O23	NH2	ARG17	H-acceptor	3.33	−0.8
	14	−6.89	1.68	6-Ring	CG1	VAL21	Pi–H	3.53	−0.5
				6-Ring	CD1	LEU496	Pi–H	4.18	−0.5
	15	−6.83	1.68	O4	NH1	ARG17	H-acceptor	2.96	−3.3
				O4	NH2	ARG17	H-acceptor	3.05	−3.0
				O15	ND2	ASN493	H-acceptor	3.09	−0.6
	16	−6.72	1.69	N2	OE1	GLN490	H-donor	3.01	−2.8
	17	−6.66	1.73	N2	OE1	GLN490	H-donor	2.95	−2.7
	18	−7.26	1.99	6-Ring	CG1	VAL21	Pi–H	3.61	−0.7
				6-Ring	CG2	VAL21	Pi–H	3.95	−0.6
	Original ligand	−8.63	1.98	O4	OE1	GLU485	H-donor	2.86	−3.5

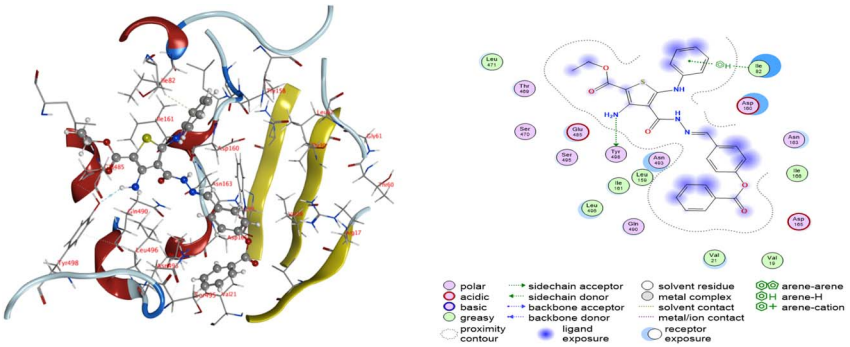

Fig. 6 3D and 2D interactions of compound **12** with the AChE target.

ppm): 122.38 (2C), 122.56 (2C), 128.68 (3C), 128.74 (2C), 128.93 (2C), 130.28 (3C), 130.30 (2C), 130.33 (2C), 131.18 (1C), 131.30 (1C), 134.04 (1C), 134.10 (1C), 153.64 (2C, 2C–O), 161.50 (2C, 2C=N), 164.78 (2C, 2C=O). Anal. calcd for $C_{28}H_{20}N_2O_4$ (448.14): C, 74.99; H, 4.50; N, 6.25%. Found: C, 74.92; H, 4.54; N, 6.29%.

*3.1.1.2 4-((2-Carbamoylhydrazineylidene)methyl)phenyl benzoate (**3**).* Beige crystals; yield 93%; m.p. = 238–240 °C. IR (ν_{max}/cm^{-1}): 3458, 3285, 3166 (NH_2, NH), 1736 (C=O_{ester}), 1687 (C=O_{amidic}), 1639 (C=N). ^{1}H NMR (400 MHz) (DMSO): δ (ppm) = 6.53 (s, 2H, NH_2), 7.31 (d, J = 8.80 Hz, 2H), 7.62 (t, J = 7.60 Hz, 2H), 7.76 (t, J = 7.60 Hz, 1H), 7.82 (d, J = 8.80 Hz, 2H), 7.88 (s, 1H, CH=N), 8.14 (d, J = 7.20 Hz, 2H), 10.29 (s, 1H, NH). ^{13}C NMR (100 MHz) (δ/ppm): 123.42 (2C), 128.97 (1C), 129.48 (2C), 130.22 (1C), 130.37 (2C), 132.42 (2C), 134.75 (1C), 151.37 (1C), 154.03 (1C), 156.88 (1C, C=O), 164.67 (1C, C=O). MS, m/z (%) 283 (M^+, 16.17%), 257 (37.78%), 244 (46.00%), 210 (42.62%), 168 (39.40%), 138 (41.06%), 131 (100.00%), 59 (71.68%). Anal. calcd for $C_{15}H_{13}N_3O_3$ (283.10): C, 63.60; H, 4.63; N, 14.83%. Found: C, 63.66; H, 4.69; N, 14.85%.

*3.1.1.3 4-((2-(4-Aminobenzoyl)hydrazineylidene)methyl) phenyl benzoate (**5**).* White crystals; yield 92%; m.p. = 281–283 °C. IR (ν_{max}/cm^{-1}): 3454, 3333 (NH_2), 3252 (NH), 1735 (C=O_{ester}), 1644 (C=O), 1604 (C=N). ^{1}H NMR (500 MHz) (DMSO): δ (ppm) = 5.82 (s, 2H, NH_2), 6.62 (d, J = 8.00 Hz, 2H), 7.35 (d, J = 8.00 Hz, 2H), 7.59 (t, J = 8.00 Hz, 2H), 7.71 (m, 3H), 7.78 (d, J = 8.00 Hz, 2H), 8.12 (d, J = 7.00 Hz, 2H), 8.46 (s, 1H, CH=N), 11.55 (s, 1H, NH). ^{13}C NMR (125 MHz) (δ/ppm): 112.66 (1C), 119.48 (1C), 122.43 (2C), 128.02 (2C), 128.78 (1C), 128.99 (3C), 129.43 (1C), 129.85 (3C), 132.64 (1C), 134.13 (1C), 145.05 (1C, C=N), 151.54 (1C, C–O), 152.37 (1C, C–NH_2), 163.14 (1C, –CONH), 164.48 (1C, –COO). Anal. calcd for $C_{21}H_{17}N_3O_3$ (359.13): C, 70.18; H, 4.77; N, 11.69%. Found: C, 70.23; H, 4.70; N, 11.66%.

*3.1.1.4 4-((2-(Phenylsulfonyl)hydrazineylidene)methyl)phenyl benzoate (**6**).* White crystals; yield 73%; m.p. = 207–209 °C. IR (ν_{max}/cm^{-1}): 3195 (NH), 1728 (C=O_{ester}), 1624 (C=N). ^{1}H NMR (500 MHz) ($CDCl_3$): δ (ppm) = 7.22–8.25 (m, 15H, aromatic-H, CH=N), 10.05 (s, 1H, NH). MS, m/z (%) 380 (M^+, 16.46%), 371 (54.79%), 358 (64.63%), 317 (61.63%), 298 (100.00%), 249 (69.37%), 118 (50.77%), 71 (53.03%). Anal. calcd for $C_{20}H_{16}N_2O_4S$ (380.08): C, 63.15; H, 4.24; N, 7.36%. Found: C, 63.10; H, 4.29; N, 7.31%.

*3.1.1.5 4-((2-Isonicotinoylhydrazineylidene)methyl)phenyl benzoate (**7**).* White crystals; yield 82%; m.p. = 250–252 °C. IR (ν_{max}/cm^{-1}): 3285 (NH), 1736 (C=O_{ester}), 1665 (C=O_{amidic}). ^{1}H NMR (400 MHz) (DMSO): δ (ppm) = 7.42 (d, J = 8.40 Hz, 2H), 7.63 (t, J = 7.60 Hz, 3H), 7.81 (t, J = 7.60 Hz, 1H), 7.85 (m, 3H), 8.15 (d, J = 7.60 Hz, 2H), 8.52 (s, 1H, CH=N), 8.79 (d, J = 5.60 Hz, 2H), 12.12 (s, 1H, NH). ^{13}C NMR (100 MHz) (δ/ppm): 120.54 (2C), 122.95 (2C), 128.59 (2C), 128.74 (1C), 129.23 (2C), 129.49 (2C), 129.84, 130.18 (2C), 132.74 (1C), 134.64 (1C), 141.43 (1C), 152.16 (1C), 162.78 (1C, C=O), 164.90 (1C, C=O). MS, m/z (%) 345 (M^+, 8.03%), 319 (31.85%), 186 (43.27%), 129 (34.15%), 74 (37.10%), 51 (55.03%), 44 (100.00%), 43 (53.56%). Anal. calcd for $C_{20}H_{15}N_3O_3$ (345.11): C, 69.56; H, 4.38; N, 12.17%. Found: C, 69.60; H, 4.35; N, 12.10%.

3.1.2 Synthesis of 4-(benzo[*d*]thiazol-2-yl)phenyl benzoate (9). A mixture of 4-substituted benzylidinemalononitrile **8** (1.37 g, 0.005 mol) and 2-aminothiophenol (0.52 mL, 0.005 mol) was dissolved in 20 mL ethyl alcohol, and then refluxed for 20 min. The resulting solid was filtered and washed with hot ethyl alcohol to yield benzothiazole derivative **9**.

Yellow crystals; yield 88%; m.p. = 148–150 °C. IR (ν_{max}/cm^{-1}): 1726 (C=O_{ester}). ^{1}H NMR (500 MHz) ($CDCl_3$): δ (ppm) = 7.37–7.42 (m, 3H), 7.51–7.55 (m, 3H), 7.64 (t, J = 8.00 Hz, 1H), 7.90 (d, J = 7.50 Hz, 1H), 8.09 (d, J = 8.00 Hz, 1H), 8.17 (d, J = 8.50 Hz, 2H), 8.22 (d, J = 7.00 Hz, 2H). ^{13}C NMR (125 MHz) (δ/ppm): 121.62 (1C), 122.41 (2C), 123.10 (1C), 125.33 (1C), 126.45 (1C), 128.62 (2C), 128.83 (2C), 129.10 (1C), 130.20 (2C), 131.05 (1C), 133.81 (1C), 134.88 (1C), 153.08 (1C, C–O), 153.71 (1C, C–N), 164.74 (1C, C=O), 167.06 (1C, S–C=N). Anal. calcd for $C_{20}H_{13}NO_2S$ (331.07): C, 72.49; H, 3.95; N, 4.23%. Found: C, 72.41; H, 3.99; N, 4.20%.

3.1.3 Synthesis of 4-(1,6-diamino-3,5-dicyano-2-oxo-1,2-dihydropyridin-4-yl)phenyl benzoate (10). A mixture of 4-substituted benzylidinemalononitrile **8** (1.37 g, 0.005 mol) and 2-cyanoacetohydrazide (0.49 g, 0.005 mol) was suspended in 20 mL dry ethyl alcohol containing piperidine (0.5 mL), and then the mixture was refluxed. After a few minutes, a precipitate was formed. The deposited compound was filtered and washed well with hot EtOH to afford compound **10**.

Beige crystals; yield 75%; m.p. > 300 °C. IR (ν_{max}/cm^{-1}): 3367–3166 ($2NH_2$), 2214 (2CN), 1737 (C=O_{ester}), 1654 (C=O_{amidic}). ^{1}H NMR (400 MHz) (DMSO): δ (ppm) = 5.68 (s, 2H,

Table 8 Interactions of tested compounds with GST targets

Receptor residues	Compound	Score (kcal mol^{-1})	RMSD (Å)	Atom of compound	Atom of receptor	Involved residue	Type of interaction	Distance (Å)	E (kcal mol^{-1})
GST residues involved:	**2**	−6.97	2.26	O22	NE2	GLN104	H-acceptor	3.08	−1.4
TYR7 TRP8 LEU10	**3**	−6.18	2.22	N3	OD1	ASN59	H-donor	3.42	−1.0
GLY12 LEU13 PHE35				N4	OD1	ASN59	H-donor	3.52	−1.1
LYS43 LEU60 GLN74				O1	NZ	LYS43	H-acceptor	3.06	−7.5
THR75 VAL76 ALA77				O15	OH	TYR118	H-acceptor	3.00	−1.5
ILE107 ILE110 PHE111				O1	NE1	TRP8	H-acceptor	3.09	−0.8
CYS113 THR114 TRP117	**4**	−6.41	1.54	O14	NE1	TRP8	H-acceptor	3.09	−0.5
TYR118 ILE168 TYR171				N23	OG1	THR114	H-acceptor	3.14	−1.0
ILE213 THR214				6-Ring	OH	TYR7	Pi–H	4.04	−0.5
GLY215 MET217	**5**	−6.38	1.69				Ligand exposure		
	6	−6.89	1.68	O5	CA	THR214	H-acceptor	3.55	−0.5
				O6	OH	TYR118	H-acceptor	2.96	−1.8
				O21	NE1	TRP8	H-acceptor	3.04	−2.9
	7	−6.59	2.27	N7	NZ	LYS50	H-acceptor	3.04	−0.5
				O20	NE1	TRP8	H-acceptor	3.06	−3.1
				O20	NZ	LYS43	H-acceptor	3.18	−1.9
	9	−6.46	1.58	6-Ring	OH	TYR7	Pi–H	3.41	−0.5
				6-Ring	NZ	LYS43	Pi–cation	3.88	−0.5
	10	−6.67	1.99	N23	OD1	ASN59	H-donor	2.98	−3.5
				O24	NE1	TRP8	H-acceptor	3.04	−2.0
				O24	NZ	LYS43	H-acceptor	2.96	−4.6
	12	−7.57	1.77	O15	NE2	GLN74	H-acceptor	3.31	−0.7
	13	−7.90	1.78	O15	NE2	GLN74	H-acceptor	3.30	−0.8
	14	−7.01	1.51	O15	N	VAL76	H-acceptor	3.12	−2.6
				S21	OH	TYR118	H-acceptor	3.57	−1.1
				S21	CA	THR214	H-acceptor	3.85	−1.1
				5-Ring	CG	LEU13	Pi–H	3.99	−0.6
				5-Ring	OH	TYR118	Pi–H	4.66	−0.5
	15	−6.93	1.76	O21	NE1	TRP46	H-acceptor	3.02	−2.9
				O21	CE	LYS50	H-acceptor	2.95	−0.9
				6-Ring	CG2	ILE110	Pi–H	4.05	−0.5
	16	−7.03	1.60	N2	O	LEU60	H-donor	3.34	−0.7
				N23	N	LEU60	H-acceptor	3.08	−1.3
				5-Ring	NZ	LYS50	Pi–cation	3.87	−2.7
				6-Ring	CG2	ILE110	Pi–H	3.92	−0.5
	17	−6.89	1.56	O15	OH	TYR118	H-acceptor	3.03	−1.1
	18	−6.59	1.73	N2	O	LEU60	H-donor	2.90	−5.7
				N35	NZ	LYS43	H-acceptor	3.37	−1.3
				6-Ring	OH	TYR7	Pi–H	4.20	−0.5
				6-Ring	OH	TYR7	Pi–H	3.55	−0.5
	Original ligand	−6.31	1.86	N3	OG1	THR114	H-donor	3.03	−1.8
				O12	NE1	TRP8	H-acceptor	2.91	−5.6
				O12	NZ	LYS43	H-acceptor	2.93	−9.7
				OE1	OH	TYR118	H-acceptor	3.09	−0.9
				O11	NZ	LYS 43	Ionic	2.98	−4.6
				O12	NZ	LYS 43	Ionic	2.93	−4.9

NH_2), 7.50 (d, J = 8.80 Hz, 2H), 7.61–7.66 (m, 4H), 7.78 (t, J = 7.60 Hz, 1H), 8.17 (d, J = 7.60 Hz, 2H), 8.50 (s, 2H, NH_2). ^{13}C NMR (100 MHz) (δ/ppm): 74.87 (1C, C–CN), 115.98 (1C, CN), 116.85 (1C, CN), 122.73 (2C), 129.21 (1C), 129.50 (3C), 130.11 (1C), 130.36 (3C), 132.63 (1C), 134.68 (1C), 152.40 (1C, C–O), 157.12 (1C, –C–NH_2), 159.21 (1C, –CO–N), 159.69 (1C, –COO), 164.77 (1C, C4 pyridine ring). Anal. calcd for $C_{20}H_{13}N_5O_3$ (371.10): C, 64.69; H, 3.53; N, 18.86%. Found: C, 64.73; H, 3.55; N, 18.80%.

3.1.4 Synthesis of thiophene derivatives 12 and 13. General procedure. A mixture of 4-((2-(2-cyanoacetyl)hydrazono)methyl) phenyl benzoate (**4**) (0.49 g, 0.005 mol), KOH (0.28 g, 0.005 mol) and phenyl isothiocyanate (0.59 mL, 0.005 mol) in DMF (15 mL) was stirred overnight, and then the α-halo derivative, namely bromoethylacetate (0.58 mL, 0.005 mol) or phenacylchloride (0.77 g, 0.005 mol), was added dropwise with stirring for 6 h. The previous mixture was placed onto ice-water with stirring, and then filtered, dried and crystallized from EtOH to afford the corresponding thiophenes **12** and **13**, respectively.

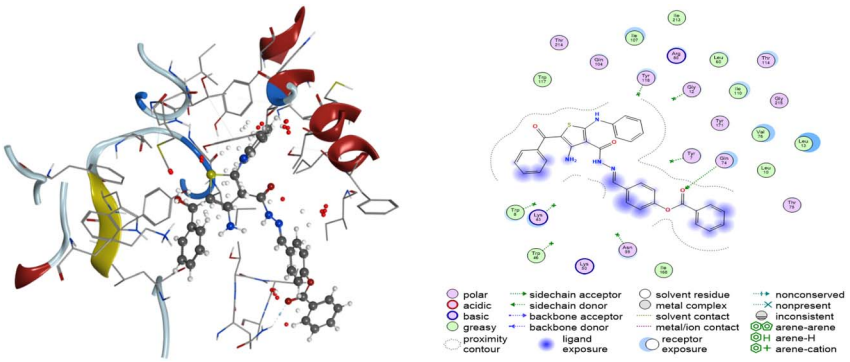

Fig. 7 3D and 2D interactions of compound **13** with the GST target.

*3.1.4.1 Ethyl-3-amino-4-(2-(4-(benzoyloxy)benzylidene) hydrazine-1-carbonyl)-5-(phenylamino)thiophene-2-carboxylate (**12**).* Yellow powder; yield 50%; m.p. = 182–184 °C. IR (ν_{max}/cm^{-1}): 3395–3243 (2NH, NH_2), 1735 (2C=O_{ester}), 1665 (C=O_{amidic}), 1601 (C=N). ^{1}H NMR (400 MHz) (DMSO): δ (ppm) = 1.22 (t, J = 7.20 Hz, 3H, CH_3), 4.15 (q, J = 7.20 Hz, 2H, CH_2), 6.69 (s, 2H, NH_2), 7.10 (t, J = 7.20 Hz, 1H), 7.36 (m, 4H), 7.63 (t, J = 7.60 Hz, 3H), 7.75–7.80 (m, 3H), 7.95 (s, 1H), 8.14 (d, J = 7.60 Hz, 2H), 8.25 (s, 1H, CH=N), 9.70 (s, 1H, NH), 11.39 (s, 1H, NH). ^{13}C NMR (100 MHz) (δ/ppm): 15.06 (1C, CH_3), 59.46 (1C, CH_2), 104.90 (1C, NH–CO–C), 120.54 (2C), 122.95 (2C), 123.11 (1C), 123.67 (1C), 124.21 (1C), 128.59 (2C), 128.74 (1C), 129.23 (1C), 129.49 (2C), 129.84 (2C), 130.18 (2C), 130.31 (1C), 132.74 (1C), 134.64 (1C, C=N), 141.43 (1C, C–O), 152.16 (1C, COOEt), 162.78 (1C, CONH), 163.95 (1C, Ph–C=O), 164.90 (1C, NH–C–S). MS, m/z (%) 528 (M^+, 18.39%), 383 (78.43%), 370 (65.00%), 305 (68.54%), 89 (40.58%), 85 (43.02%), 57 (92.59%), 55 (100.00%). Anal. calcd for $C_{28}H_{24}N_4O_5S$ (528.15): C, 63.62; H, 4.58; N, 10.60%. Found: C, 63.66; H, 4.60; N, 10.55%.

*3.1.4.2 4-((2-(4-Amino-5-benzoyl-2-(phenylamino)thiophene-3-carbonyl)hydrazono)methyl)phenyl benzoate (**13**).* Yellow crystals; yield 85%; m.p. = 256–258 °C. IR (ν_{max}/cm^{-1}): 3448, 3347, 3298, 3231 (NH_2, 2NH), 1734 (C=O_{ester}), 1671 (C=O), 1628 (C=N). ^{1}H NMR (500 MHz) ($CDCl_3$): δ (ppm) = 7.10–8.19 (m, 30H, aromatic-H, CH=N, NH_2), 10.08 (s, 1H, NH), 10.53 (s, 1H, NH). ^{13}C NMR (δ/ppm): 98.46 (1C), 101.68 (1C), 120.13 (2C), 122.74 (2C), 124.90 (2C), 127.29 (2C), 127.31 (2C), 128.45 (2C), 128.77 (2C), 129.66 (2C), 129.83 (2C), 130.01 (1C), 130.78 (1C), 132.02 (1C), 132.23 (1C), 139.05 (1C), 140.90 (1C), 145.64 (1C), 146.65 (1C), 150.90 (1C, C=O), 155.40 (1C, C=O), 162.98 (1C, S–C–N), 187.06 (1C, C=O). MS, m/z (%) 560 (M^+, 3.21%), 448 (95.90%), 377 (100.00%), 351 (67.70%), 318 (43.27%), 293 (46.97%), 104 (45.27%), 76 (33.67%). Anal. calcd for $C_{32}H_{24}N_4O_4S$ (560.15): C, 68.56; H, 4.31; N, 9.99%. Found: C, 68.57; H, 4.38; N, 9.97%.

3.1.5 Synthesis of 4-((2-(4-amino-3-phenyl-2-thioxo-2,3-dihydrothiazole-5-carbonyl)hydrazineylidene)methyl)phenyl benzoate (14). A mixture of equimolar amounts of cyanoacetyl hydrazone **4** (0.49 g, 0.005 mol), phenyl isothiocyanate (0.59 mL, 0.005 mol) and elemental sulfur (0.16 g, 0.005 mol) was dissolved in 15 mL dimethylformamide containing 0.5 mL triethylamine and refluxed for 3 h. Then, the reaction mixture was poured onto ice-water containing drops of dil. HCl for neutralization. The resulting precipitate was collected by filtration, and then recrystallized from EtOH, giving **14**.

Brown powder; yield 63%; m.p. = 250–252 °C. IR (ν_{max}/cm^{-1}): 3441 (br, NH, NH_2), 1732 (C=O_{ester}), 1626 (C=O_{amidic}), 1599 (C=N). ^{1}H NMR (500 MHz) (DMSO): δ (ppm) = 7.07–7.35 (m, 10H), 7.52 (d, J = 9.00 Hz, 2H), 7.65 (d, J = 9.00 Hz, 2H), 7.89 (s, 2H, NH_2), 8.05 (s, 1H, CH=N), 10.33 (s, 1H, NH). ^{13}C NMR (100 MHz) (δ/ppm): 74.01 (1C, S–C–CO), [120.19 (1C), 123.19 (1C), 129.52 (3C), 130.35 (2C), 130.48 (2C), 132.52 (1C), 133.61 (1C), 135.42 (1C), 136.23 (1C), 137.00 (1C), 137.54 (1C), 139.84 (1C), 142.57 (1C) (Ar–C)], 143.06 (1C, C=N), 145.08 (1C, C–O), 152.61 (1C, –C–NH_2), 172.31 (1C, Ph–C=O), 174.13 (1C, –HN–C=O), 177.72 (1C, C=S). Anal. calcd for $C_{24}H_{18}N_4O_3S_2$ (474.08): C, 60.74; H, 3.82; N, 11.81%. Found: C, 60.69; H, 3.88; N, 11.85%.

3.1.6 Synthesis of 4-((2-(2-(4-oxothiazolidin-2-ylidene) acetyl)hydrazineylidene)methyl)phenyl benzoate (15). Thioglycolic acid (0.35 mL, 0.005 mol) was added to a solution of **4** (0.49 g, 0.005 mol) in 15 mL glacial acetic acid. The reaction mixture was allowed to cool, and then poured onto crushed ice after being refluxed for 4 h. The furnished product was separated by filtration and recrystallized from EtOH to produce **15**.

Yellow powder; yield 67%; m.p. = 244–246 °C. IR (ν_{max}/cm^{-1}): 3364, 3201 (2NH), 1731 (C=O_{ester}), 1670 (C=O_{cyclic}), 1623 (C=O_{amidic}), 1599 (C=N). ^{1}H NMR (400 MHz) (DMSO): δ (ppm) = 3.02 (s, 2H, CH_2), 5.34 (s, 1H, methylidene H), 7.21–8.15 (m, 10H, aromatic-H, CH=N), 9.92 (s, 1H, NH), 11.11 (s, 1H, NH). MS, m/z (%) 381 (M^+, 42.03%), 335 (56.64%), 182 (100.00%), 156 (77.79%), 126 (63.02%), 117 (64.88%), 96 (69.17%), 75 (62.54%). Anal. calcd for $C_{19}H_{15}N_3O_4S$ (381.08): C, 59.83; H, 3.96; N, 11.02%. Found: C, 59.89; H, 3.90; N, 11.06%.

3.1.7 Synthesis of arylidene 16, 2-iminochromene 17 and benzochromene 18. General procedure. In ethanol (20 mL) containing a catalytic quantity of piperidine, a mixture of **4** (0.49 g, 0.005 mol) and furfural (0.42 mL, 0.005 mol), salicylaldehyde (0.52 mL, 0.005 mol) or 2-hydroxy-1-naphthaldehyde (0.86 g, 0.005 mol) was refluxed for 1–2 h. The obtained precipitate on heating was collected by filtration and washed with boiling ethyl alcohol to furnish **16**, **17** and **18**, respectively.

*3.1.7.1 4-((2-(2-Cyano-3-(furan-2-yl)acryloyl)hydrazineylidene) methyl)phenyl benzoate (**16**).* Reddish brown powder; yield 82%; m.p. > 300 °C. IR (ν_{max}/cm^{-1}): 3286 (br, NH), 2208 (CN), 1732 (C=O$_{ester}$), 1686 (C=O$_{amidic}$), 1599 (C=N). ^{1}H NMR (400 MHz) (DMSO): δ (ppm) = 7.35–8.17 (m, 15H, aromatic-H, CH=N, CH=C, NH). MS, *m*/*z* (%) 385 (M$^+$, 8.38%), 149 (39.62%), 102 (44.77%), 97 (26.70%), 89 (100.00%), 86 (48.40%), 58 (72.59%), 57 (68.36%). Anal. calcd for $C_{22}H_{15}N_3O_4$ (385.11): C, 68.57; H, 3.92; N, 10.90%. Found: C, 68.50; H, 3.95; N, 10.97%.

*3.1.7.2 4-((2-(2-Imino-2H-chromene-3-carbonyl) hydrazineylidene)methyl)phenyl benzoate (**17**).* Yellow crystals; yield 65%; m.p. = 216–218 °C. IR (ν_{max}/cm^{-1}): 3304 (2NH), 1726 (C=O$_{ester}$), 1675 (C=O$_{amidic}$), 1598 (C=N). ^{1}H NMR (400 MHz) ($CDCl_3$): δ (ppm) = 7.17 (d, J = 8.00 Hz, 1H), 7.23–7.67 (m, 9H, aromatic-H), 7.87 (d, J = 8.40 Hz, 2H), 8.20 (d, J = 7.60 Hz, 2H), 8.31 (s, 1H, CH=N), 8.77 (s, 1H, CH$_{pyran}$), 13.63 (s, 1H, NH). ^{13}C NMR (100 MHz) (δ/ppm): 115.37 (2C), 118.69, 119.54, 122.72 (2C), 124.44, 128.53 (2C), 129.00 (2C), 129.71, 129.81 (2C), 131.98, 132.80, 133.17, 143.18, 145.60, 147.63, 150.91, 153.81 (1C, C–O), 157.56 (1C, C=NH), 159.11 (1C, C=O). MS, *m*/*z* (%) 411 (M$^+$, 9.92%), 339 (37.33%), 328 (24.12%), 145 (37.12%), 122 (41.63%), 85 (53.82%), 74 (61.59%), 68 (100.00%). Anal. calcd for $C_{24}H_{17}N_3O_4$ (411.12): C, 70.07; H, 4.17; N, 10.21%. Found: C, 70.02; H, 4.19; N, 10.28%.

*3.1.7.3 4-((2-(3-Imino-3H-benzo[f]chromene-2-carbonyl) hydrazineylidene)methyl)phenyl benzoate (**18**).* Yellow crystals; yield 78%; m.p. = 210–212 °C. IR (ν_{max}/cm^{-1}): 3279 (2NH), 1737 (C=O$_{ester}$), 1672 (C=O$_{amidic}$), 1599 (C=N). ^{1}H NMR (400 MHz) ($CDCl_3$): δ (ppm) = 7.20–8.53 (m, 16H, aromatic-H, CH=N), 8.71 (s, 1H, CH$_{pyran}$), 9.75 (s, 1H, NH), 13.60 (s, 1H, NH). ^{13}C NMR (100 MHz) (δ/ppm): [112.81 (1C), 115.63 (1C), 122.04 (3C), 126.20 (1C), 128.64 (4C), 128.90 (1C), 129.08 (1C), 129.32 (1C), 129.72 (2C), 130.23 (1C), 131.66 (4C), 133.75 (1C), 134.77 (1C) (Ar–C)], 148.48 (1C, C=N), 152.61 (1C, C–O pyran), 153.58 (1C, C–O), 158.09 (1C, C=NH), 159.40 (1C, Ph–C=O), 164.85 (1C, –NH–C=O). Anal. calcd for $C_{28}H_{19}N_3O_4$ (461.14): C, 72.88; H, 4.15; N, 9.11%. Found: C, 72.85; H, 4.18; N, 9.16%.

3.2 Pesticidal bioassays

3.2.1 Pest collection and rearing. Laboratory susceptible and homogeneous strains of *S. littoralis* (Boisd.) and *T. urticae* (Koch) were provided by the Plant Protection Research Institute, ARC, Mansoura Branch, Egypt. The egg clusters of *S. littoralis* were kept in a climatic control chamber until hatching at 25 °C, 70% RH, and a photoperiod of 14L:10D. The fourth instar larvae used in the bioassay experiment were obtained by feeding the generated larvae on castor leaves.[47] Also, under laboratory sets (25 ± 2 °C and 60 ± 5% RH), *T. urticae* (Koch) was reared and colonized on castor oil plant leaves.[2,55]

3.2.2 Leaf dipping bioassays. The sixteen newly synthesised compounds were emulsified in water using 0.3% Tween 80. Subsequently, five serially diluted concentrations of each treatment were prepared and immediately applied. The leaf-dip technique was used to evaluate the activity of the tested derivatives against 4th instar larvae of *S. littoralis*[47] and adult females of *T. urticae*.[2,55] The control treatment was prepared using only 0.3% Tween 80. Each treatment and control were performed in triplicate, and the mortality was recorded 24 and 72 h after exposure for both pests.[2,55]

3.2.3 Biochemical investigation of pests. The enzyme activities of both pests were estimated after the application of the sublethal concentrations (LC_{50}) of the outstanding toxicants. After a day of application, the surviving individuals were gathered, weighed, and kept at 4 °C until estimation. Untreated pests were prepared and designated as the control.[2] The frozen individuals were homogenated in phosphate buffer (pH 6.8) and centrifuged at 5000 rpm for 10 min under cooling conditions. The filtrate was poured in an Eppendorf tube and stored at −20 °C in a refrigerator as an enzyme source. Each enzyme assay was replicated three times, and its activity was assessed colorimetrically. The activities of aspartate transaminase (AST) and alanine transaminase (ALT) were measured at 520 nm,[56] and acetyl choline esterase (AChE)[57] and glutathione S-transferase (GS-T) were measured at 540 nm (ref. 58) at the Plant Protection Research Institute's analysis unit, A.R.C.

3.3 Docking study

To correlate the *in vitro* biological findings with the binding affinity of the compounds, molecular docking was conducted against the AChE and GST target proteins. This process involves the computational alignment of two molecules, the substrate and its target receptor active site, to determine the optimal three-dimensional configuration that maximizes their interaction. To investigate the potential of the constituents, molecular docking analyses were conducted using the MOE software.[59,60] The receptor proteins in this research, acetylcholinesterase, and glutathione S-transferase, were downloaded from the RCSB PDB (**https://www.rcsb.org/**) with PDB IDs of 6XYS and 8UDB for AChE and GST, respectively.[61] AChE and GST were selected as established target enzymes due to their well-characterized roles in detoxification and neural function in arthropods, including the studied pest species. Currently, structural and mechanistic data for more species-specific targets in *S. littoralis* and *T. urticae* are limited. Importantly, the relevance of these targets in our test species was experimentally cross-validated by measuring their activity post-treatment, thereby supporting the biological significance of the docking findings. The co-crystallized ligand and investigated compounds were prepared in MOE through 3D protonation and energy minimization, and stored in MDB format. Target protein data from the Protein Data Bank (PDB) were refined in MOE to rectify structural flaws. Hydrogen atoms were added, solvent molecules removed, and energy minimized to optimize the final protein structures for docking analysis. The potential binding sites on the target protein were identified using the Site Finder tool in MOE, which detects pockets based on alpha sphere placement, and docking was performed using the triangle matcher placement method, followed by refinement with the default parameters optimized. The top-ranked site was selected as the active site for docking. A docking grid was automatically generated around this site, with the default radius (~10 Å) encompassing the entire binding pocket. Docking tests were conducted using the triangle

matcher and refining approaches. Following the completion of the docking operations, the resulting poses were assessed. The most suitable poses, demonstrating the best acceptable rmsd_refine ratios and retaining identical interaction modes to the native ligand, were selected for further analysis.

3.4 Statistical analysis

According to Abbott's formula, the mortality rates were calculated and corrected.[62] The results of the bioassay test and insect enzyme activity were subjected to analysis of variance (ANOVA), least significant difference (LSD) and Duncan's multiple range test at $p \leq 0.05$ and the standard error (SE) was calculated using the CoHort software (CoHort, 2004). The LC_{50} and LC_{90} values were estimated by Finney's mortality regression lines[63] and Sun's equation was used to compute the toxicity index.[64]

4. Conclusion

A series of new hydrazones and heterocycles incorporating the phenyl benzoate moiety was felicitously prepared *via* condensation reactions of the versatile scaffolds 4-formylphenyl benzoate (**1**), cyanoacetyl hydrazone **4** and 4-substituted benzylidinemalononitrile **8** with various organic reagents. The structures of the newly constructed derivatives (**2–18**) were verified using different spectral and analytical data. The sixteen synthesized compounds were evaluated for their pesticidal effectiveness compared with the standard references methomyl and pyridaben. Among the test derivatives, compounds **3**, **4**, **10**, **12**, **13**, **16** and **17** were the most potent against the 4th instar larvae of *S. littoralis* and adult females of *T. urticae*. The mechanism of action of the most potent compounds was clarified through estimation of some key enzymes, and also with the aid of *in silico* studies.

Conflicts of interest

There are no conflicts to declare.

Data availability

The data supporting this article, including [IR, ^{1}H NMR, ^{13}C NMR, and mass spectra of the newly synthesized phenylbenzoate derivatives and D interactions of the synthesized compounds with AChE and GST target] have been included as part of the SI. See DOI: **https://doi.org/10.1039/d5ra03713a**.

References

1 W. S. Hamama, G. G. El-Bana, M. E. H. Mostafa and H. H. Zoorob, *J. Heterocycl. Chem.*, 2019, **56**, 239–250.
2 H. M. Metwally, E. Abdel-Latif, M. E. Mostafa and G. E. Said, *J. Heterocycl. Chem.*, 2025, **62**, 345–361.
3 N. Bajsa, E. Fabiano and F. Rivas-Franco, *Environ. Sustainability*, 2023, **6**, 121–133.
4 P. Devendar and G.-F. Yang, *Sulfur Chemistry*, 2017, pp. 35–78.
5 M. Khedr and H. El-Kawas, *J. Entomol.*, 2013, **10**, 170–181.
6 R. El-Sharkawy and R. R. Abdullah, *J. Plant Prot. Pathol.*, 2020, **11**, 249–252.
7 E. A. Ghaith, H. A. Ali, M. A. Ismail, A. E.-A. S. Fouda and M. Abd El Salam, *BMC Chem.*, 2023, **17**, 144.
8 Z.-H. Chen, W.-S. Li, Z.-Y. Zhang, H. Luo, J.-R. Wang, H.-Y. Zhang, Z.-R. Zeng, B. Chen, X.-W. Li and Y.-W. Guo, *Org. Lett.*, 2021, **23**, 5621–5625.
9 W. J. Wu, M. M. Li, B. Liu and Y. Wu, *Eur. J. Org Chem.*, 2019, 3169–3173.
10 E. Abdel-Galil, E. B. Moawad, A. El-Mekabaty and G. E. Said, *Synth. Commun.*, 2018, **48**, 2083–2092.
11 X. Yao, R. Zhang, B. Lv, W.-W. Wang, Z. Liu, Z. Hu and D. Li, *Adv. Agrochem*, 2023, **2**, 154–162.
12 E. Abdel-Galil, M. M. Girges and G. E. Said, *ChemistrySelect*, 2020, **5**, 3075–3079.
13 G. E. Said, M. Tarek, A. S. Al-Wasidi, A. M. Naglah, A. A. Almehizia and T. K. Khatab, *J. Mol. Struct.*, 2024, **1311**, 138462.
14 E. Pivovarova, A. Climova, M. Świątkowski, M. Staszewski, K. Walczyński, M. Dzięgielewski, M. Bauer, W. Kamysz, A. Krześlak and P. Jóźwiak, *Int. J. Mol. Sci.*, 2022, **23**, 9844.
15 E. Abdel-Galil, E. B. Moawad, A. El-Mekabaty and G. E. Said, *J. Heterocycl. Chem.*, 2018, **55**, 1092–1100.
16 A. C. Tripathi, S. J. Gupta, G. N. Fatima, P. K. Sonar, A. Verma and S. K. Saraf, *Eur. J. Med. Chem.*, 2014, **72**, 52–77.
17 O. Devinyak, B. Zimenkovsky and R. Lesyk, *Curr. Top. Med. Chem.*, 2012, **12**, 2763–2784.
18 G. M. Reddy, J. R. Garcia, V. H. Reddy, A. M. de Andrade, A. Camilo Jr, R. A. P. Ribeiro and S. R. de Lazaro, *Eur. J. Med. Chem.*, 2016, **123**, 508–513.
19 A. R. Shaikh, M. Farooqui, R. Satpute and S. Abed, *J. Drug Delivery Ther.*, 2018, **8**, 424–428.
20 A. Al-Mulla, *Der Pharma Chem.*, 2017, **9**, 141–147.
21 E. A. Ghareeb, N. F. Mahmoud, E. A. El-Bordany and E. A. El-Helw, *Bioorg. Chem.*, 2021, **112**, 104945.
22 F. Song, D. Liu, X. Huo and D. Qiu, *Arch. Pharm.*, 2022, **355**, 2100277.
23 G. E. Said, M. M. Girges and E. Abdel-Galil, *Russ. J. Gen. Chem.*, 2021, **91**, 2527–2538.
24 R. Gujjarappa, A. K. Kabi, S. Sravani, A. Garg, N. Vodnala, U. Tyagi, D. Kaldhi, S. Gupta and C. C. Malakar, in *Nanostructured Biomaterials: Basic Structures and Applications*, Springer, 2022, pp. 101–134.
25 K. Kant, C. K. Patel, S. Banerjee, P. Naik, A. K. Atta, A. K. Kabi and C. C. Malakar, *ChemistrySelect*, 2023, **8**, e202303988.
26 R. Gujjarappa, N. Vodnala and C. Malakar, *ChemistrySelect*, 2020, **5**, 8745–8758.
27 M. Singh, R. Jamra, A. K. Paul, C. C. Malakar and V. Singh, *Asian J. Org. Chem.*, 2022, **11**, e202100653.
28 N. Aljaar, C. C. Malakar, J. r. Conrad, S. Strobel, T. Schleid and U. Beifuss, *J. Org. Chem.*, 2012, **77**, 7793–7803.
29 S. Çağlar Yavuz, S. Akkoç, B. Türkmenoğlu and E. Sarıpınar, *J. Heterocycl. Chem.*, 2020, **57**, 2615–2627.
30 Z. M. Nofal, A. M. Srour, N. M. Mansour and S. S. A. El-Karim, *Polycyclic Aromat. Compd.*, 2022, **42**, 5411–5421.
31 P. Devendar and G.-F. Yang, *Sulfur Chemistry*, 2019, pp. 35–78.

32 Y. Wang, S. Guo, L. Yu, W. Zhang, Z. Wang, Y. R. Chi and J. Wu, *Chin. Chem. Lett.*, 2024, **35**, 108207.
33 W. Q. Li, Z. J. Zhang, X. Nan, Y. Q. Liu, G. F. Hu, H. T. Yu, X. B. Zhao, D. Wu and L. T. Yan, *Pest Manage. Sci.*, 2014, **70**, 667–673.
34 M. Liu, Y. Wang, W.-z. Wangyang, F. Liu, Y.-l. Cui, Y.-s. Duan, M. Wang, S.-z. Liu and C.-h. Rui, *J. Agric. Food Chem.*, 2010, **58**, 6858–6863.
35 Z.-B. Yang, D.-Y. Hu, S. Zeng and B.-A. Song, *Bioorg. Med. Chem. Lett.*, 2016, **26**, 1161–1164.
36 J. Wu, B. A. Song, D. Y. Hu, M. Yue and S. Yang, *Pest Manage. Sci.*, 2012, **68**, 801–810.
37 M. Aly, M. M. Ibrahim, A. Okael and Y. Gherbawy, *Russ. J. Bioorg. Chem.*, 2014, **40**, 214–227.
38 Z. Che, S. Zhang, Y. Shao, L. Fan, H. Xu, X. Yu, X. Zhi, X. Yao and R. Zhang, *J. Agric. Food Chem.*, 2013, **61**, 5696–5705.
39 L. Prapanthadara, N. Promtet, S. Koottathep, P. Somboon and A. Ketterman, *Insect Biochem. Mol. Biol.*, 2000, **30**, 395–403.
40 B. S. K. Aktar, Y. Sicak, G. Tatar and E. E. Emre, *Turk. J. Chem.*, 2022, **46**, 236–252.
41 R. T. von Stein, K. S. Silver and D. M. Soderlund, *Pestic. Biochem. Physiol.*, 2013, **106**, 101–112.
42 Ł. Popiołek, *Biomed. Pharmacother.*, 2021, **141**, 111851.
43 S. K. Ramadan, D. R. A. Haleem, H. S. Abd-Rabboh, N. M. Gad, W. S. Abou-Elmagd and D. S. Haneen, *RSC Adv.*, 2022, **12**, 13628–13638.
44 Y. P. Agrawal, M. Y. Agrawal and A. K. Gupta, *Chem. Biol. Drug Des.*, 2015, **85**, 172–180.
45 S. M. H. Sanad and A. E. M. Mekky, *J. Iran. Chem. Soc.*, 2020, **17**, 3299–3315.
46 X. Yao, R. Zhang, B. Lv, W.-W. Wang, Z. Liu, Z. Hu and D. Li, *Adv. Agrochem*, 2023, **2**, 154–162.
47 M. E.-H. Mostafa, A. Abdelmonem, F. Z. El-Ablack, M. Abdel-Mogib and S.-E. N. Ayyad, *Sci. J. Damietta Fac. Sci.*, 2023, **13**, 39–47.
48 P. T. Giboney, *Am. Fam. Physician*, 2005, **71**, 1105–1110.
49 A. Kinareikina and E. Silivanova, *Toxics*, 2023, **11**, 47.
50 M. Krátký, Š. Štěpánková, K. Konečná, K. Svrčková, J. Maixnerová, M. Švarcová, O. Janďourek, F. Trejtnar and J. Vinšová, *Pharmaceuticals*, 2021, **14**, 1229.
51 M. Krátký, K. Svrčková, Q. A. Vu, Š. Štěpánková and J. Vinšová, *Molecules*, 2021, **26**, 989.
52 M. J. Mphahlele, E. N. Agbo, S. Gildenhuys and I. B. Setshedi, *Biomolecules*, 2019, **9**, 736.
53 P. C. Agu, C. A. Afiukwa, O. U. Orji, E. M. Ezeh, I. H. Ofoke, C. O. Ogbu, E. I. Ugwuja and P. M. Aja, *Sci. Rep.*, 2023, **13**, 13398.
54 M. Mohanty and P. S. Mohanty, *Monatsh. Chem.*, 2023, **154**, 683–707.
55 V. Dittrich, *J. Econ. Entomol.*, 1962, **55**, 644–648.
56 V. Harold, *Practical Clinical Biochemistry*, Gulab, 1975.
57 D. R. Simpson, D. L. Bull and D. A. Lindquist, *Ann. Entomol. Soc. Am.*, 1964, **57**, 367–371.
58 W. H. Habig, M. J. Pabst and W. B. Jakoby, *J. Biol. Chem.*, 1974, **249**, 7130–7139.
59 A. P. Tolstova, A. A. Makarov and A. A. Adzhubei, *J. Chem. Inf. Model.*, 2024, **64**, 918–932.
60 Y. Wang, W. Huang, S. Zheng, L. Wang, L. Zhang and X. Pei, *Sci. Rep.*, 2024, **14**, 1422.
61 F. Nachon, T. L. Rosenberry, I. Silman and J. L. Sussman, *Molecules*, 2020, **25**, 1198.
62 W. S. Abbott, *J. Econ. Entomol.*, 1925, **18**, 265–267.
63 D. Finney, *Probit Analysis*, Cambridge University Press, London, 1971, p. 633.
64 Y.-P. Sun, *J. Econ. Entomol.*, 1950, **43**, 45–53.